Hypervelocity Stars

Manfred Hanke,

guided by Prof. Heber,
Astronomical Institute of the University of Erlangen-Nuremberg, Bamberg

September 2006

Abstract

In this project, the kinematics of the recently discovered hypervelocity stars HVS4 – HVS7, whose stellar types and therefore distances are not yet known, is investigated numerically. It is also shown, how the distances and maximal ages can be estimated. Finally, different models for the Galactic potential are discussed.

According to Hill's process of production of HVS via the central supermassive black hole, a trajectory originating in the Galactic center can be found for each HVS (with currently unknown proper motion), both if they are main sequence stars with solar (or lower) metalicity in large distances or alternatively nearer horizontal branch stars. All HVSs are unbound to the Milky Way. These results are independent of the model for the Galactic potential that is used for the numerical computation.

Contents

1 Hypervelocity stars: an overview

High-velocity or runaway stars, that result from supernova explosions in binary systems or close encounters of stars, have velocities typically lower than 200 km s^{-1} and are therefore still gravitationally bound to the Galaxy.
Hypervelocity stars (HVSs) however exceed their corresponding Galactic escape velocity. They have already been predicted in 1988 by Hills [1], assuming a supermassive black hole in the Galactic center, whose tidal forces might disrupt a closely passing binary system and accelerate one member to velocities up to 4 000 km s^{-1}. Yu & Tremaine considered in 2003 [2] further mechanisms and estimated their production rate of HVSs, namely close encounters of single stars (which is quite inefficient) and interactions of a single star with a binary black hole (which would produce by one order of magnitude more HVSs than Hills' process, but is not very likely to be realized in the Milky Way).

The first HVS was discovered in 2005 by Brown et al. [3] in their survey of blue horizontal branch stars using the Sloan Digital Sky Survey (SDSS). After two discoveries at the Astronomical Institute of the University of Erlangen-Nuremberg, HE 0437-5439 by Edelmann et al. 2005 [4] and US 708 by Hirsch et al. 2005 [5], an explicit survey of HVSs by the group of Brown has revealed 4 more such stars until now: HVS4 and HVS5 [6], HVS6 and HVS7 [7], cf. table 1.

One can of course easily measure the radial velocity from the Doppler-shift in the spectrum; HVS1 – HVS7 have 530 km $s^{-1} \leq v_{\rm rad} \leq$ 860 km s^{-1}, cf. table 1. Trustable measurements of proper motions for the determination of the tangential velocity are not available, as their values are most likely of the order of 1 mas yr^{-1} due to their probably large distance – and therefore below the accuracy that can currently be obtained.

Table 1: currently known HVSs

#	catalog name / coordinates	$v_{\rm rad}$/(km s^{-1})	$l_{\rm gal}$/deg	$b_{\rm gal}$/deg
HVS1	SDSS J090745.0+0245071	+853	227.3	31.3
HVS2	US 708 ≡ SDSS J093320.86+441705.4	+708s	176.0	47.1
HVS3	HE 0437-54393	+723	263.0	-40.9
HVS4	SDSS J091301.0+305120	+603	194.8	42.6
HVS5	SDSS J091759.5+672238	+543	146.3	38.7
HVS6	SDSS J110557.45+093439.5	+606	243.1	59.6
HVS7	SDSS J113312.12+010824.9	+531	263.8	57.9

This project is organized as follows:
Section 2 describes, how a star's distance can be calculated from its mass, effective temperature and surface gravity. The latter two quantities can be obtained from fits of the measured spectra to those of simulated stellar model atmospheres. From the assumption of known stellar types, the mass can furthermore be determined by comparison with simulated stellar evolution tracks. The distances and maximal ages are estimated in detail for HVSs #4 – #7
Section 3 shows, how (and which) proper motions of the HVSs can be found, such that numerically computed trajectories in the Galactic potential originate from the Galactic center – according to Hills' production process of HVSs by the supermassive central black hole. From these orbits, one will be able to draw the conclusion, that some HVSs had to be ejected from the Galactic center very soon after their births.
In section 4, other models for the Galactic potential are investigated numerically with respect to their influence on the results for the HVSs. It will be shown, that there exist several models which describe the kinematics of the HVSs equally well.

2 Estimation of the distances and maximal ages

2.1 Calculation of the distance from the stellar flux

The flux of light f_V arriving at earth at the wavelength $\lambda_V = 550$ nm can be calculated on the one hand from the flux F_V emanating from the star's surface (which can be taken from a table of computed model atmospheres [8], if effective temperature $T_{\rm eff}$, surface gravity g and metalicity are known), and on the other hand from the apparent visual magnitude (the absolute calibration factor can be found for example in [9]):

$$f_V \;=\; \frac{\theta^2}{4} F_V = \pi \frac{R^2}{d^2} F_V \;=\; 3.607 \cdot 10^{-9} \, \frac{\rm erg}{\rm cm^2 \, s \, \mathring{A}} \cdot 10^{-0.4V}$$

If the mass M is known, the distance can be calculated from the surface gravity $g = \frac{GM}{R^2}$:

$$d\left(V,\, M,\, T_{\rm eff},\, \log \tfrac{g}{\rm cm\,s^{-2}}\right) \;=\; \sqrt{\pi \, \frac{GM}{g} \, \frac{F_V}{f_V}} \;=\; 1.11\,{\rm kpc} \, \sqrt{\frac{M}{M_\odot} \, \frac{\rm cm\,s^{-2}}{g} \, \frac{F_V(T_{\rm eff}, \log(\frac{g}{\rm cm\,s^{-2}}))}{10^8 \, \frac{\rm erg}{\rm cm^2\,s\,\mathring{A}}} \, 10^{0.4V}} \qquad (1)$$

(The constants $G = 6.67 \cdot 10^{-5} \, \frac{\rm cm^3}{\rm kg\,s^2}$, $M_\odot = 2 \cdot 10^{30}\,{\rm kg}$ and $1\,{\rm kpc} = 3.085 \cdot 10^{21}\,{\rm cm}$ have been used.)

Effective temperature $T_{\rm eff}$ and surface gravity g of a star can be obtained from fits of its measured spectrum to simulated stellar model atmospheres. Heber obtained following results for the HVSs (private communication):

Table 2: apparent visual magnitude and Heber's results for effective temperature and surface gravity of the HVSs

#	V/mag	$T_{\rm min}$	T	$T_{\rm max}$	$\log(\frac{g_{\rm max}}{\rm cm\,s^{-2}})$	$\log(\frac{g}{\rm cm\,s^{-2}})$	$\log(\frac{g_{\rm min}}{\rm cm\,s^{-2}})$
HVS4	18.56	13 490 K	13 900 K	14 380 K	4.20	4.00	3.80
HVS5	18.03	11 880 K	12 300 K	12 730 K	4.34	4.14	3.94
HVS6	19.22	11 880 K	12 300 K	12 730 K	4.52	4.32	4.12
HVS7	17.90	12 490 K	12 900 K	13 320 K	3.89	3.69	3.49

2.2 Estimation of the mass and maximal age by main sequence evolution tracks

A star on the main sequence evolves on a certain track (depending on its mass) in a $\log g$ – $\log T_{\rm eff}$ diagram, which is similar to the $\log L$ – $\log T$ diagram of Hertzsprung and Russell, due to the following identity:

$$\log(g/({\rm cm\,s^{-2}})) = \log(M/M_\odot) + 4\log(T/K) - \log(L/L_\odot) - 10.6049,$$

as $L = \sigma T^4 \cdot 4\pi R^2$ and $g = \frac{GM}{R^2}$ (The constants $\sigma = 5.67 \cdot 10^{-8}\,\frac{\rm Ws}{\rm m^2\,K^4}$ and $L_\odot = 3.827 \cdot 10^{26}\,{\rm W}$ have been used).

These tracks have been calculated e.g. by Schaller, Schaerer et al. for different metalicities ([10], [11], [12]). (As the metal content of the stellar population in the Galactic center is unknown, three different metalicities Z were considered: solar $Z_\odot = 0.020$, sub-solar $Z = 0.008$ and twice solar $Z = 0.040$.)
Respecting the error bars (see tab. 2), one can estimate masses and upper limits for the HVSs' ages.

2.2.1 Solar metalicity $Z_\odot = 0.020$

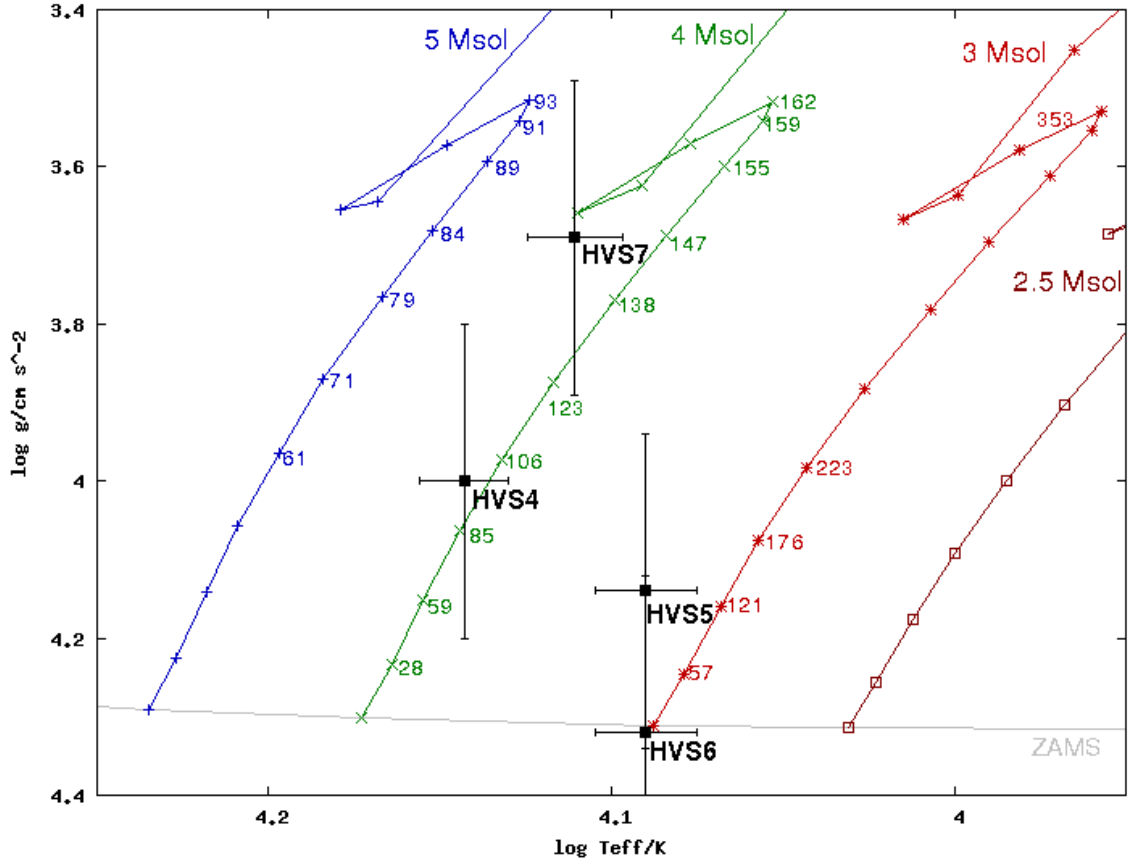

Figure 1: evolution tracks of main sequence stars with Z=0.020 (after Schaller et al. [10])
The numbers indicate the evolution time in units of Myr.

Table 3: masses and maximal ages of the HVSs, if they are main sequence stars with $Z = 0.020$, estimated from the corresponding evolution tracks (figure 1)

#	M	$T_{\rm max}$
HVS4	$3.7\,M_\odot \le 4.2\,M_\odot \le 4.7\,M_\odot$	110 Myr
HVS5	$2.8\,M_\odot \le 3.3\,M_\odot \le 3.7\,M_\odot$	200 Myr
HVS6	$2.6\,M_\odot \le 3.0\,M_\odot \le 3.4\,M_\odot$	120 Myr
HVS7	$3.8\,M_\odot \le 4.4\,M_\odot \le 4.9\,M_\odot$	165 Myr

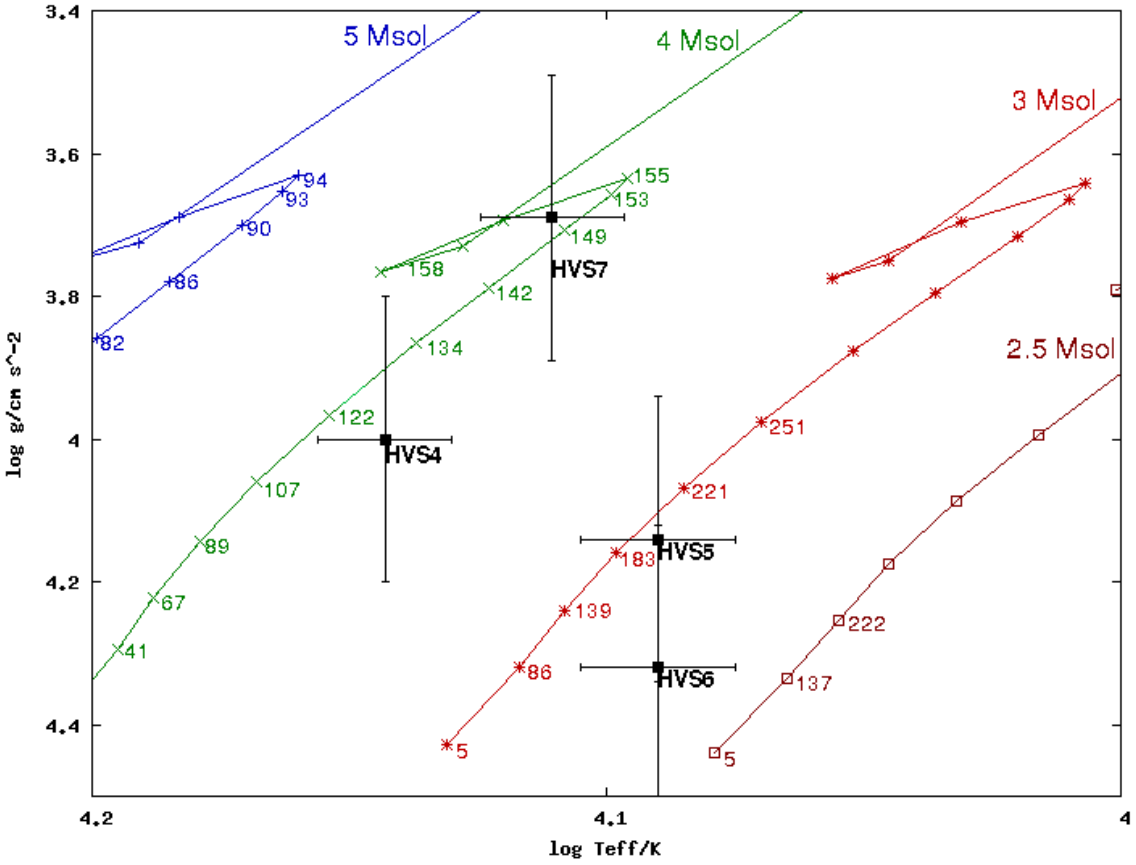

Figure 2: evolution tracks of main sequence stars with Z=0.008 (after Schaerer et al. [11]) The numbers indicate the evolution time in units of Myr. (see section 2.2.2)

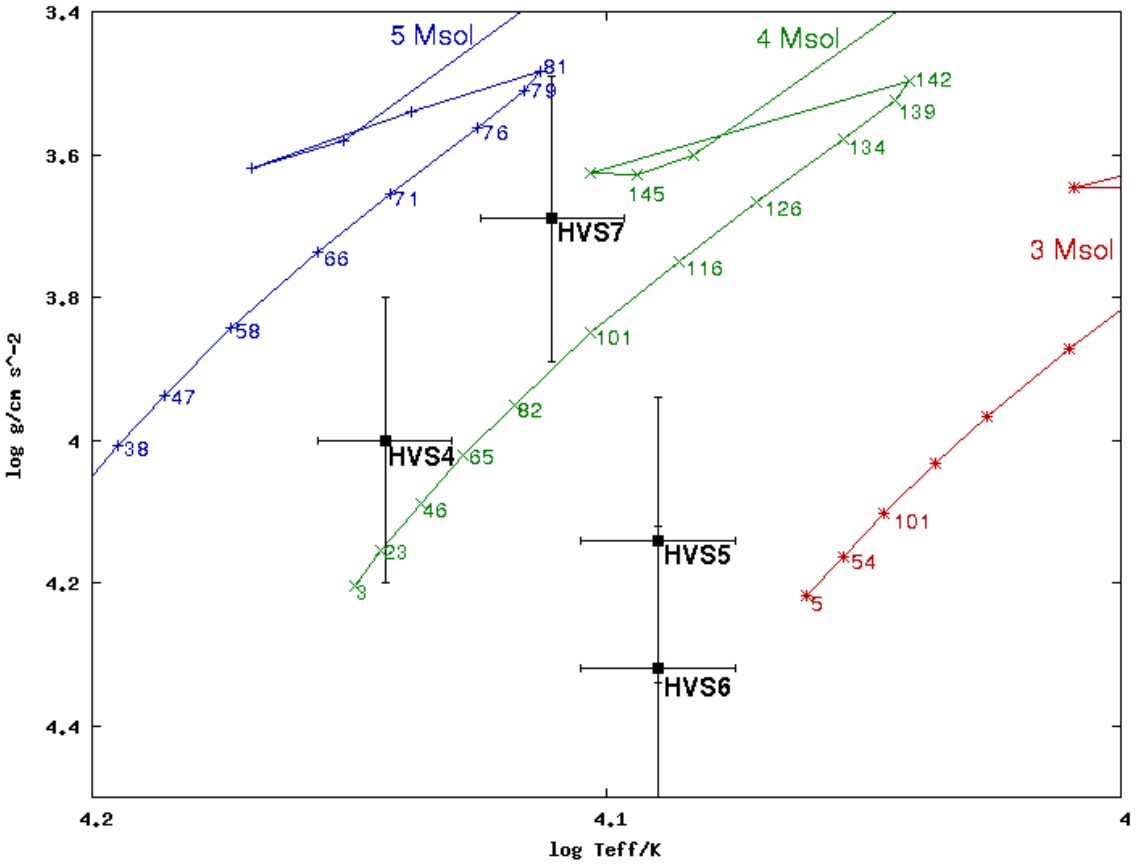

Figure 3: evolution tracks of main sequence stars with Z=0.040 (after Schaerer et al. [12]) The numbers indicate the evolution time in units of Myr. (see section 2.2.3)

2.2.2 Metalicity $Z = 0.008 < Z_\odot$

Table 4: masses and maximal ages of the HVSs, if they are main sequence stars with $Z = 0.008$, estimated from the corresponding evolution tracks (figure 2)

#	M	$T_{\max}$
HVS4	$3.4\,M_\odot \leq 3.8\,M_\odot \leq 4.4\,M_\odot$	140 Myr
HVS5	$2.6\,M_\odot \leq 2.9\,M_\odot \leq 3.4\,M_\odot$	240 Myr
HVS6	$2.4\,M_\odot \leq 2.7\,M_\odot \leq 3.2\,M_\odot$	220 Myr
HVS7	$3.6\,M_\odot \leq 4.1\,M_\odot \leq 4.5\,M_\odot$	160 Myr

For metalicities below the solar value of $Z_\odot = 0.020$ (here $Z = 0.008$), the corresponding evolution tracks (figure 2) give slightly lower masses and therefore higher maximal ages (see table 4 in comparison with table 3).

2.2.3 Metalicity $Z = 0.040 > Z_\odot$

Table 5: masses and maximal ages of the HVSs, if they are main sequence stars with $Z = 0.040$, estimated from the corresponding evolution tracks (figure 3)

#	M	$T_{\max}$
HVS4	$3.8\,M_\odot \leq 4.3\,M_\odot \leq 4.8\,M_\odot$	70 Myr
HVS5	$3.0\,M_\odot \leq 3.4\,M_\odot \leq 3.8\,M_\odot$	100 Myr
HVS6	$2.8\,M_\odot \leq 3.1\,M_\odot \leq 3.6\,M_\odot$	50 Myr
HVS7	$3.9\,M_\odot \leq 4.5\,M_\odot \leq 5.1\,M_\odot$	150 Myr

If the HVSs had metalicities above the solar value ($Z = 0.040$ in figure 3), their masses would be slightly higher, but their maximal ages would be drastically lower (table 5) than in the solar case (table 3).

2.2.4 Summary of the metalicities

Higher metalicities in the stellar evolution model require larger stellar masses and therefore shorter evolution times. Within the considered range, the masses vary at most by 10%. As only the square root of the mass enters in the calculation of the distance (eq. 1), the metalicity leads to an error of only 5% in the distance, which is definitely less than the error from the uncertainty in T_{eff} and $\log g$.
The dependence of the maximal age on the mass is however much stronger, this quantity is therefore very sensitive on the underlying model.

2.3 Mass of horizontal branch stars

Unfortunately, it is not even clear that the HVSs HVS4 – HVS7 are main sequence stars. From their position in the $\log g$ – $\log T_{\text{eff}}$ diagram, they could be horizontal branch (HB) stars as well (see figure 4, showing the zero age HB and the terminal age HB, which would be horizontal in a H.-R.-diagram).
Main sequence stars gain their energy from hydrogen-fusion. Stars on the horizontal branch are, after their phase on the red giant branch, burning helium in a core of threshold mass of 0.5 $M_\odot$. In this time, the star evolves from the ZAHB towards the TAHB.
As the hydrogen-burning shell is very thin, one can assume 0.5 $M_\odot$ as canonical mass of all HB-stars.
The age of such an evolved star is much longer than for a main sequence star with more than 3 $M_\odot$ and is likely to exceed 1000 Myr.

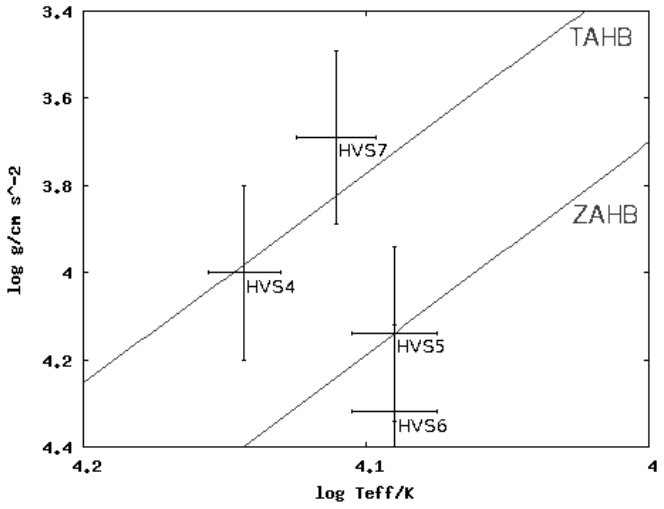

Figure 4: location of the HB in the $\log g$ – $\log T_{\text{eff}}$ diagram

2.4 Estimated range of distances of the HVSs

The flux $F_V(T_{\text{eff}},\ \log(\frac{g}{\text{cm s}^{-2}}))$ at the stellar surface can be looked up in a table of computed model atmospheres [8]. Interpolation gives the following values, which are needed to calculate the distances of the HVSs by equation 1 (see table 2):

$$F_V(13\,900\,\text{K},\ 4.00) = 10^{7.568344}\,\frac{\text{erg}}{\text{cm}^2\,\text{s}\,\mathring{\text{A}}}$$
$$F_V(12\,300\,\text{K},\ 4.14) = 10^{7.475668}\,\frac{\text{erg}}{\text{cm}^2\,\text{s}\,\mathring{\text{A}}}$$
$$F_V(12\,300\,\text{K},\ 4.32) = 10^{7.475582}\,\frac{\text{erg}}{\text{cm}^2\,\text{s}\,\mathring{\text{A}}}$$
$$F_V(12\,900\,\text{K},\ 3.69) = 10^{7.513050}\,\frac{\text{erg}}{\text{cm}^2\,\text{s}\,\mathring{\text{A}}}$$

The minimal distance is obtained from minimal M, minimal $T_{\rm eff}$ and maximal g – and vice versa, of course. For the calculation of table 6, the values given in table 2 and the masses discussed in sections 2.2 and 2.3 were used:

Table 6: distances of the HVSs, depending on the underlying model

$$d_{\rm min}\left(V,\ M_{\rm min},\ T_{\rm min},\ \log(\frac{g_{\rm max}}{\rm cm\,s^{-2}})\right)/{\rm kpc}\ <\ d\left(V,\ M,\ T,\ \log(\frac{g}{\rm cm\,s^{-2}})\right)/{\rm kpc}\ <$$
$$d_{\rm max}\left(V,\ M_{\rm max},\ T_{\rm max},\ \log(\frac{g_{\rm min}}{\rm cm\,s^{-2}})\right)/{\rm kpc}$$

	main sequence			horizontal
#	$Z = 0.008$	$Z_\odot = 0.020$	$Z = 0.040$	branch
HVS4	$50 < 68 < 95$	$52 < 72 < 99$	$53 < 73 < 100$	$19 < 25 < 32$
HVS5	$26 < 36 < 50$	$27 < 38 < 53$	$28 < 39 < 53$	$11 < 15 < 19$
HVS6	$35 < 49 < 69$	$37 < 51 < 71$	$38 < 52 < 73$	$16 < 21 < 27$
HVS7	$51 < 70 < 95$	$52 < 73 < 99$	$53 < 74 < 101$	$19 < 25 < 32$

As the distances depend strongly on the underlying model, all computations in the following section 3.2 have been performed for assumed heliocentric distances 15 kpc $\le d <$ 100 kpc of the HVSs. It will be shown that nevertheless general conclusions can be drawn.

3 Back-tracing to the Galactic center

3.1 Introduction

Equatorial coordinates are given by right ascension RA and declination δ. δ is the angle in north direction above the celestial equator, which is perpendicular to Earth's axis of rotation. δ stays therefore constant for a geocentric observer. RA is the angle on the celestial equator from the vernal equinox point to the object in east direction. Being closely related to the geocentric angle from the south point, which changes with 360°/24 h, RA is given directly in hours rather than in degrees. Astronomical catalogue names often indicate these coordinates; e.g. HVS4, which is SDSS J091301.0+305120, has RA = $09^{\rm h}\ 13^{\rm min}\ 01.0^{\rm s}$, $\delta = +30°\ 51'\ 20''$. Velocities are given by proper motions μ_α and μ_δ which are the angular velocities in RA and δ (the tangential velocity is therefore $\vec{v}_{\rm t} = d \cdot \vec{\mu}$), and the heliocentric radial velocity $v_{\rm rad}$, which has been corrected for Earth's motion and rotation.

As mentioned briefly in section 1, only one component of each HVS's space velocity – namely the radial velocity from the spectrum's Doppler-shift – is known. One can now vary for each star the two components of the proper motion such that its trajectory has hit the Galactic center (within 10 pc) in the past. After conversion of coordinates and velocities to the Galactocentric restframe (by the program `obs2gal_db`, which determines the angles between the star and the Galactic north pole and center and uses the distance and velocity of the sun in the Milky Way), the program `ORBIT6` of Odenkirchen & Brosche [13] integrates the orbit in the (smooth) Galactic potential of Allen & Santillán [14] (eq. 2) in equidistant time steps. (Here, $\Delta t = 0.01$ Myr was used.)

The potential consists of a spherical central mass component (bulge) Φ_1, a disk component Φ_2 and a spherical halo component Φ_3. In Galactic cylindrical coordinates ρ, φ, z (with $r = \sqrt{\rho^2 + z^2}$), they have the simple form

$$\begin{aligned}
\Phi_1(r) &= -\frac{M_1}{\sqrt{r^2 + b_1^2}} \\
\Phi_2(\rho, z) &= -\frac{M_2}{\sqrt{\rho^2 + (a_2 + \sqrt{z^2 + b_2^2})^2}} \\
\Phi_3(r) &= -\frac{M_3 \cdot (\frac{r}{a_3})^{2.02}}{[1 + (\frac{r}{a_3})^{1.02}] \cdot r} - \frac{M_3}{1.02 a_3}\left[\ln\left[1 + (\frac{x}{a_3})^{1.02}\right] - \frac{1.02}{[1 + (\frac{x}{a_3})^{1.02}]}\right]_{x=r}^{x=100\,{\rm kpc}}
\end{aligned} \qquad (2)$$

The parameters $M_1 = 606.0\,M_{\rm gal}$ (1 Galactic mass unit $M_{\rm gal} = \frac{100\,{\rm km^2\,s^{-2}}\cdot 1\,{\rm kpc}}{G} = 2.32 \cdot 10^7\,M_\odot$), $b_1 = 0.3873$ kpc; $M_2 = 3\,690.0\,M_{\rm gal}$, $a_2 = 5.3178$ kpc, $b_2 = 0.2500$ kpc and $M_3 = 4\,615.0\,M_{\rm gal}$, $a_3 = 12.0$ kpc had been fitted by Allen & Santillán to reproduce the Galactic rotation curve (see [14]).

As the HVSs are so fast, they are hardly deflected by the Galactic potential. The trajectory's minimal distance to the Galactic center as a function of the proper motions has therefore a simple minimum that can easily be found, see figure 5.

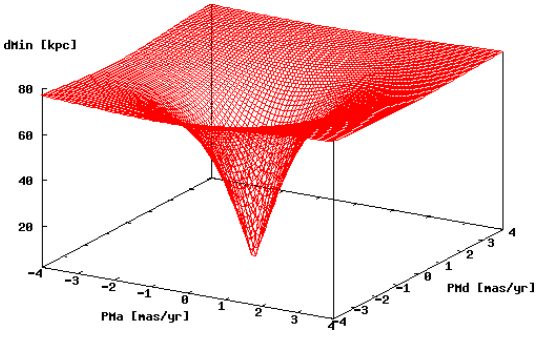

→ Figure 5: minimal distance of HVS4's trajectory depending on its proper motion (assuming a present distance of 75 kpc)

3.2 Analysis of the HVSs #4 – #7

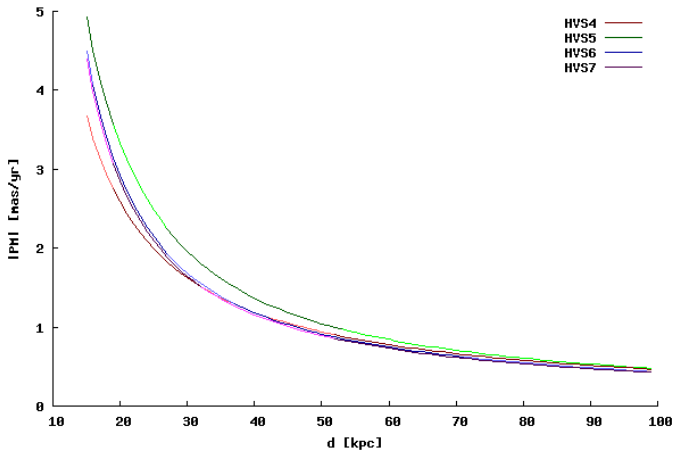

Figure 6: predicted proper motions of the HVSs (provided that they come from the Galactic center)

The computed proper motions behave nearly reciprocal to the assumed distance, see figure 6.

Unfortunately, the proper motions are mostly too low to be be measured with current precision. (Today, 2.5 - 5 mas/yr accuracy is possible in a short time span of 1-2 years.)
In this way, HVS5 could be confirmed or ruled out to be a main sequence star the most easily, see table 7.

Table 7: PMs of HVSs being HB-stars

	$\frac{d}{\text{kpc}}$	$\frac{\mu_\alpha}{\text{mas/yr}}$	$\frac{\mu_\delta}{\text{mas/yr}}$	$\frac{\lvert\vec{\mu}\rvert}{\text{mas/yr}}$
HVS4	25	-1.06	-1.69	1.99
HVS5	15	-2.97	-3.94	4.76
HVS6	21	-2.52	-1.03	2.72
HVS7	32	-1.30	-0.78	1.52

The result for the proper motions agrees with the fact that the current space velocity $v(d) = \sqrt{v_\text{t}(d)^2 + v_\text{rad}^2}$ is hardly dependent on the heliocentric distance (see figure 7). The ejection velocity (i.e. space velocity at the closest approach to the Galactic center) varies only within 6% (see figure 9).

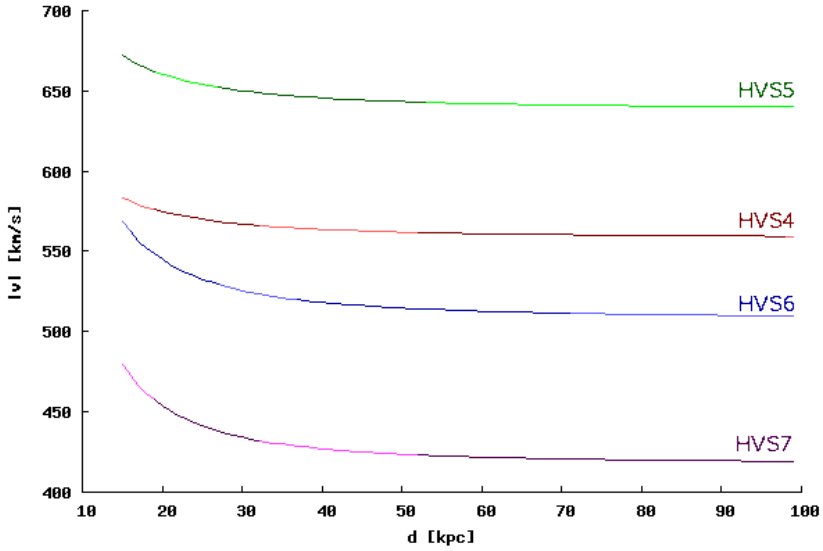

Figure 7: predicted current space velocities of the HVSs (provided that they come from the Galactic center)

HVS5 should have the largest space velocity of round 650 km/s, HVS4 has about 560 km/s, and the space velocities of HVS6 and HVS7 are approximately 515 km/s and 420 km/s respectively (see figure 7).

HVS5 and HVS4 are clearly unbound to the Galaxy, as the escape velocity (see figure 8) is less than 560 km/s for galactocentric distances larger than 6.4 kpc. HVS6 is also unbound, as $v_\text{esc}(d_\text{gal} > 10\,\text{kpc}) < 520$ km/s, and so is HVS7 due to $v_\text{esc}(d_\text{gal} > 29\,\text{kpc}) < 420$ km/s.
(In fact, the escape velocity is not a function of d_gal alone, but rather both ρ and z, as the Galactic potential is not spherical symmetric. The fact that all HVSs are unbound can be seen more clearly from the ejection velocities.)

→ Figure 8: escape velocity $v_\text{esc}(\rho, 0) = \sqrt{2|\Phi(\rho, 0)|}$ in the Galactic plane ($z = 0$), according to equation 2. ($v_\text{esc}(\rho, z)$ is anyway dominated by $\Phi_3(r)$ at large r.)

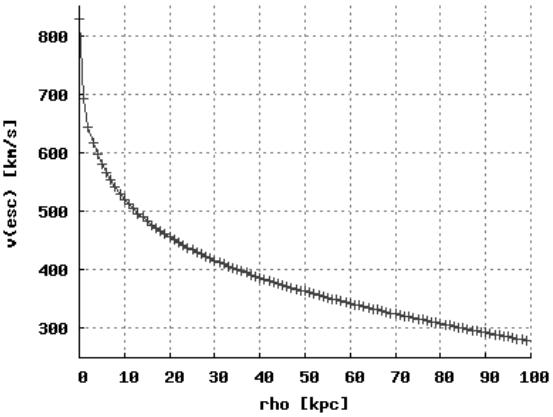

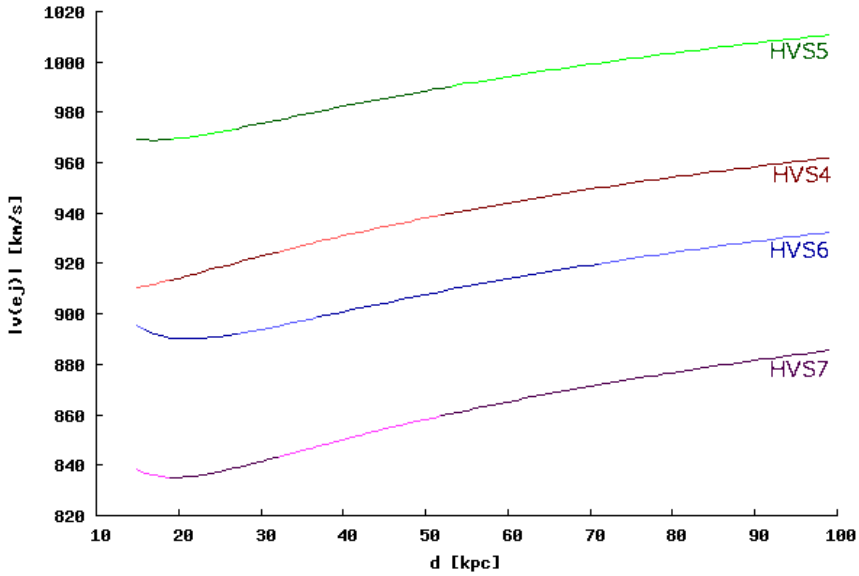

Figure 9: predicted ejection velocities of the HVSs (provided that they come from the Galactic center)

From the ejection velocities (see figure 9), one can determine whether a star is bound to the Galaxy or not, as the escape velocity at the center is (by equation 2) $v_{\mathrm{esc}}(0,0) = \lim_{\rho \to 0} \sqrt{2|\Phi(\rho,0)|} = 828.1\ \frac{\mathrm{km}}{\mathrm{s}}$. All HVSs are thus unbound.

In the following subsections, the travel time from the Galactic center will be investigated as a function of heliocentric distance (like before). As the HVSs' trajectories are hardly deflected by the Galactic potential due to their high velocities, the travel times depend in very good approximation linearly on the distance.

3.2.1 HVS4

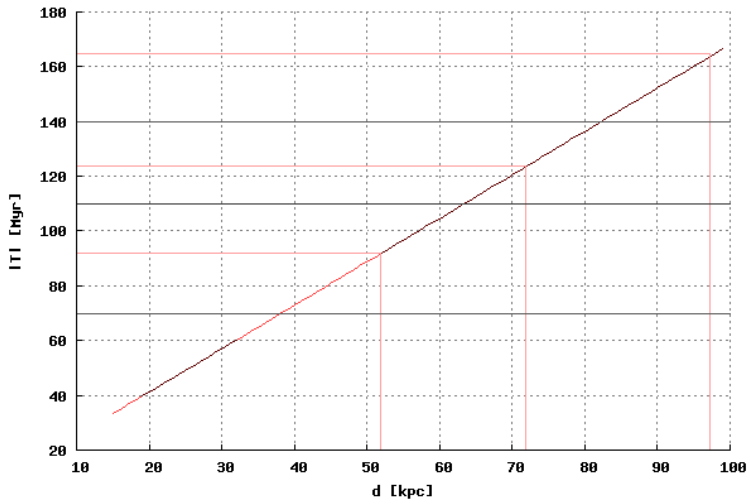

$T_{\max}(Z = 0.008) = 140$ Myr

$T_{\max}(Z_\odot = 0.020) = 110$ Myr

$T_{\max}(Z = 0.040) = 70$ Myr

Figure 10: travel time of HVS4 from the Galactic center with horizontal lines indicating maximal ages

Brown et al. assume in their paper [6] (where they reported their discovery of HVS4 and HVS5), that HVS4 is a 75 kpc distant B8-star or a 20 kpc distant blue horizontal branch star. For the first interpretation, they assume $M = 4\,M_\odot$ and $Z = 0.020$, such that Schaller's evolution tracks [10] give a full main sequence lifetime of 160 Myr, which they call consistent with their estimated travel time from the Galactic center of 130 Myr.
One can however deduce from HVS4's position in the $\log g - \log T_{\mathrm{eff}}$ diagram (figure 1), that this upper limit is too high and that HVS4 can have spent at most 110 Myr yet on the main sequence (cf. table 3). This would rule out the possibility of larger heliocentric distances than 63 kpc (see figure 10), as the travel time cannot exceed the lifetime – provided that the HVS-producing interaction with the central black hole had no influence on the stellar evolution.
According to table 6, a distance of 52 kpc is still possible for HVS4, but if this were true, this would mean that HVS4 has been kicked out of the Galactic center very soon after its birth. So HVSs might also give some information about the formation of stars in the neighbourhood of the supermassive central black hole!
Of course, if another model (other metalicities, see sections 2.2.2, 2.2.3) is used, the constraints are different: $Z = 0.008$ ($\Rightarrow T \leq 140$ Myr) would allow $d < 83$ kpc, while $Z = 0.04$ ($\Rightarrow T \leq 70$ Myr) would restrict to $d < 39$ kpc. The latter case is certainly impossible, as HVS4's distance is at least 50 kpc, if it is a main sequence star.
However, if HVS4 is a horizontal branch star, it would have needed 49 Myr to propagate from the Galactic center, if its heliocentric distance is now 25 kpc. This is possible in any case for an an HB star.

3.2.2 HVS5

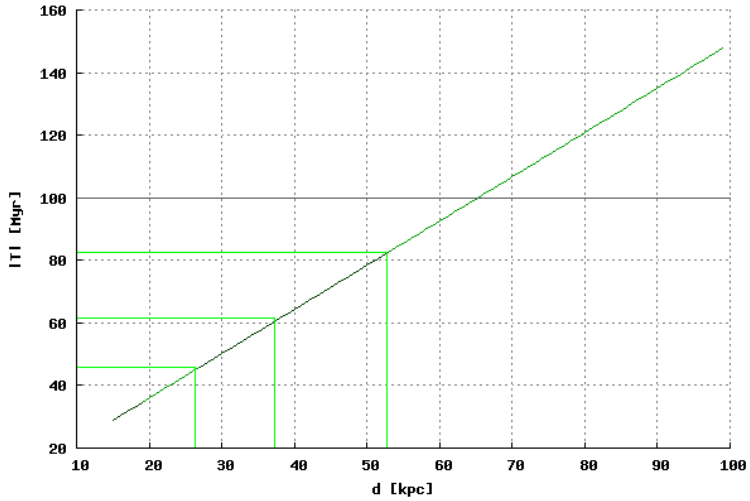

$[\, T_{\max}(Z = 0.008) = 240 \text{ Myr} \,]$

$[\, T_{\max}(Z_\odot = 0.020) = 200 \text{ Myr} \,]$

(which are both not shown here)

$T_{\max}(Z = 0.040) = 100$ Myr

Figure 11: travel time of HVS5 from the Galactic center with horizontal line indicating maximal age for $Z = 0.040$

Brown et al. assume in [6] furthermore, that HVS5 is a 55 kpc distant 4 $M_\odot$-B8-star with full main sequence lifetime of 160 Myr and estimated travel time from the Galactic center of 90 Myr.
The more detailed analysis of section 2.2 has shown, that its mass is even smaller and the main sequence lifetime therefore even larger ($T < 200$ Myr for $Z = Z_\odot$). Even the strongest constraint from the metalicity $Z = 0.040$, $T < 100$ Myr could be satisfied by $d < 66$ kpc. The origin of HVS5 in the Galactic center is thus consistent if it is a main sequence star as well as if it is an horizontal branch star.

3.2.3 HVS6

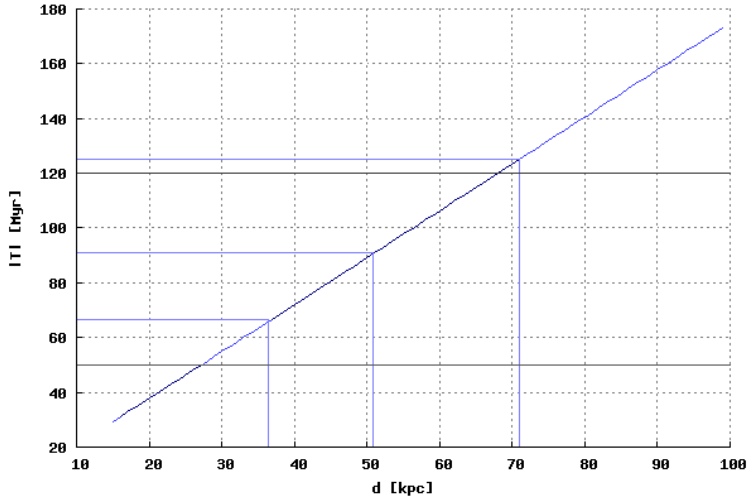

$[\, T_{\max}(Z = 0.008) = 220 \text{ Myr} \,]$
(which is off scale in this plot)

$T_{\max}(Z_\odot = 0.020) = 120$ Myr

$T_{\max}(Z = 0.040) = 50$ Myr

Figure 12: travel time of HVS6 from the Galactic center, horizontal lines: maximal ages for $Z = 0.020$ / $Z = 0.008$

In the paper [7] (where the discovery of HVS6 and HVS7 is reported), Brown et al. consider HVS6 to be either a 75 kpc distant 3 $M_\odot$-B9 main sequence star with 350 Myr full main sequence lifetime and 160 Myr travel time from the Galactic center or a 30 kpc distant blue HB-star.
The analysis of section 2.2.1 has shown that HVS6 is at most 120 Myr old, although its mass could really be 3 $M_\odot$. From figure 12, one can therefore conclude that HVS6's distance must not exceed 68 kpc, if its travel time should be consistent with its maximal age. This is possible both for a main sequence star and – as always – within the horizontal branch scenario.

3.2.4 HVS7

HVS7 is assumed by Brown et al. in [7] to be a 55 kpc distant 4 $M_\odot$ B7-star with a full main sequence lifetime of 160 Myr and travel time from the Galactic center of 120 Myr or alternatively a 15 kpc distant HB-star.
The calculations leading to table 6 yielded even larger distances (from 52 kpc up to 99 kpc). The maximal age was estimated to 165 Myr (table 3), almost independently of the metalicity model (table 4, 5), as HVS7 is in any case near the end of its main sequence lifetime. This needs $d < 82$ kpc to be consistent with its travel time (figure 13). If HVS7 is a main sequence star, it had not much time to travel to the central black hole, it was on the contrary more probably formed in its neighbourhood!

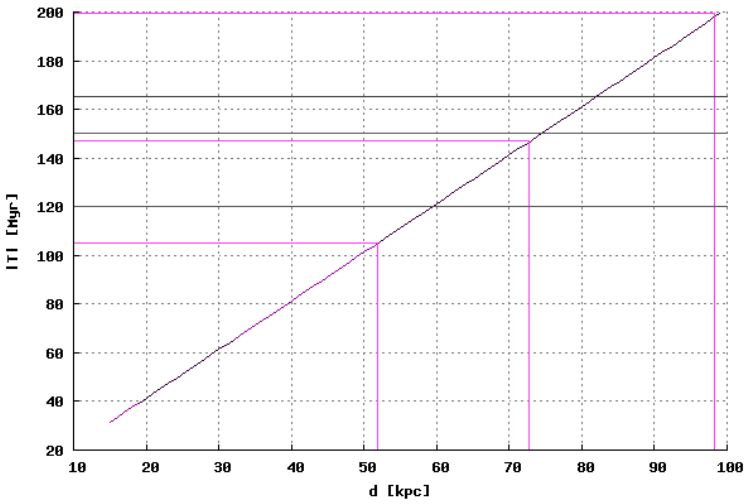

$T_{\max}(Z_\odot = 0.020) = 165$ Myr

$T_{\max}(Z = 0.008) = 160$ Myr

$T_{\max}(Z = 0.040) = 150$ Myr

Figure 13: travel time of HVS7 from the Galactic center with horizontal lines indicating maximal ages

It was shown that from the assumption of unaffected $Z = 0.020$ main sequence stars, HVSs #4 and #7 had to hurry to reach their current position in consistence with their proper lifetime. Models with lower Z would soften the constraints, but it had to be discussed if lower metalicities in the Galactic center are realistic.

3.3 Analysis of other stars with high velocities (investigated by Hirsch)

Heiko Hirsch, who discovered HVS2 (see [5]), is currently investigating further stars from the SDSS. A list of HB stars with high radial velocities (from $+253\,\frac{\mathrm{km}}{\mathrm{s}}$ to $+618\,\frac{\mathrm{km}}{\mathrm{s}}$) was received through private communication and analyzed kinematically for their possible origin in the Galactic center, which was possible for every star with positive radial velocity. (For each star, only the distance calculated from the canonical HB-mass of $0.5\,M_\odot$ and the means of the fits of $\log T_{\mathrm{eff}}$ and $\log g$ was considered.)

Table 8: radial velocity, assumed distance, proper motions, current velocity, ejection velocity and travel time for 48 stars investigated by Heiko Hirsch

SDSS name (coordinates)	v_{rad} [km s^{-1}]	V [mag]	T_{eff} [1000 K]	$\log(\frac{g}{\mathrm{cm\,s^{-2}}})$	$\Rightarrow\ d$ [kpc]	μ_α [mas/yr]	μ_δ [mas/yr]	v [km s^{-1}]	v_{ej} [km s^{-1}]	T Myr
J0320-0606	+375	17.5	12.4	4.45	8	7.05	-0.88	384.0	778.4	32.0
J0811+0534	+283	18.1	11.9	4.94	6	-4.96	-5.16	206.4	696.7	40.3
J0811+0649	+322	18.7	11.7	4.80	9	-7.52	-1.61	339.1	748.3	28.8
J0823+0558	+305	18.9	10.6	4.88	8	-1.77	-3.85	196.5	704.8	49.6
J0824+0610	+304	16.7	11.3	4.45	5	-3.65	-5.67	208.3	695.4	39.5
J0825+0822	+419	18.4	12.5	4.85	8	-2.84	-3.40	325.0	750.0	36.0
J0831+2727	+318	18.8	12.4	4.55	13	-1.64	-3.42	302.9	758.3	50.9
J0842+0834	+388	17.7	11.7	4.91	5	-6.23	-4.87	314.0	733.1	30.2
J0843+0459	+347	17.9	11.7	4.38	10	-1.83	-2.89	234.2	722.3	49.5
J0843+0753	+346	18.7	15.5	4.67	13	-1.16	-2.44	234.9	732.6	58.7
J0844+0232	+360	17.9	13.4	4.25	13	-1.20	-2.18	233.6	731.1	57.8
J0845+0724	+345	18.5	12.2	4.59	11	-1.66	-2.86	237.4	726.2	51.5
J0845+0836	+281	17.4	13.9	5.37	**3**	**-9.43**	**-9.70**	214.7	685.6	32.8
J0846+0900	+349	18.7	11.5	4.63	11	-1.76	-2.95	247.2	729.2	50.0
J0848+2855	+273	17.9	12.3	4.74	7	-3.37	-6.18	249.7	718.4	40.8
J0851+3039	+327	18.6	10.9	3.44	39	-0.21	-1.18	284.3	792.7	119.3
J0854+3217	+258	17.2	12.4	4.74	**5**	**-5.69**	**-8.67**	258.5	713.3	35.1
J0900+3413	+318	18.9	11.7	4.54	13	-1.07	-3.27	273.7	747.9	55.4
J0904+1001	+253	19.2	12.9	4.84	12	-1.36	-3.08	150.7	705.2	67.5
J0905+0554	+400	18.1	13.3	3.75	26	-0.56	-1.27	274.3	770.7	84.4
J0905+0747	+348	16.3	12.1	4.80	**3**	**-13.34**	**-6.90**	301.8	717.7	26.5
J0907+3659	+378	18.3	11.4	4.03	18	-1.27	-2.60	370.4	797.5	53.6
J0915+3712	+353	17.7	12.3	4.71	7	-6.15	-6.70	378.5	770.7	29.8
J0916+0833	+256	18.0	13.0	4.99	6	-4.61	-5.58	175.3	687.5	43.4
J0918+0901	+283	18.1	11.8	3.59	28	-0.05	-1.30	154.7	741.1	125.6
J0928+0834	+379	18.5	14.1	4.78	10	-3.24	-2.82	291.5	740.9	41.4
J0932-0021	+270	16.9	14.5	3.88	14	-1.40	-2.27	139.4	705.7	73.1
J0935+0920	+341	17.9	11.5	4.89	6	-7.42	-4.49	286.3	722.3	31.9
J0943+1054	+462	17.4	11.1	4.33	8	-5.96	-2.68	409.5	788.8	29.2
J0959+1009	+340	17.1	13.3	4.48	7	-6.23	-3.65	287.7	727.8	34.1

continuation of table 8

SDSS name (coordinates)	$v_{\rm rad}$ [km s^{-1}]	V [mag]	$T_{\rm eff}$ [1000 K]	$\log(\frac{g}{\rm cm\,s^{-2}})$	$\Rightarrow d$ [kpc]	μ_α [mas/yr]	μ_δ [mas/yr]	v [km s^{-1}]	$v_{\rm ej}$ [km s^{-1}]	T Myr
J1001+0039	+325	18.2	11.5	3.58	29	-0.67	-1.10	188.5	747.0	109.6
J1009+1020	+262	18.3	11.8	4.70	9	-3.98	-3.70	191.9	701.0	47.0
J1009+1039	+282	18.0	11.2	3.68	23	-0.97	-1.58	181.5	735.8	93.3
J1049+4254	+276	19.0	13.3	5.01	9	-5.77	-3.86	344.6	760.5	34.7
J1102+0100	+382	17.2	16.5	4.23	12	-5.19	-1.32	336.4	754.9	33.5
J1120+0415	+358	18.9	12.8	3.92	30	-1.12	-1.04	259.3	766.3	88.3
J1122+4207	+328	20.1	12.3	5.18	12	-4.99	-2.52	401.1	793.8	34.6
J1144−0129	+382	18.4	13.7	3.97	23	-1.48	-1.18	272.4	761.0	70.5
J1158+0733	+322	17.1	12.2	4.40	7	-2.02	-4.33	219.2	707.5	44.0
J1159+0645	+267	18.0	12.0	4.43	10	-5.36	-2.14	248.1	715.7	37.7
J1200+0733	+365	18.5	12.5	4.66	10	-6.71	-1.34	375.2	769.4	28.8
J1205+4804	+364	15.5	12.7	4.92	**2**	**-88.63**	**13.36**	878.1	1 087.4	9.8
J1251+1516	+405	19.4	23.2	5.05	17	-3.88	-0.92	427.3	811.1	34.9
J1252+1417	+255	17.9	12.5	4.58	9	-8.89	-0.99	348.2	747.4	25.5
J1314+1459	+284	18.7	10.6	3.59	33	-1.26	-0.88	275.1	773.1	87.0
J1319−0114	+313	16.4	17.6	4.60	**6**	**-31.50**	**9.12**	842.4	1 058.1	9.2
J1326+0355	+369	18.9	15.2	4.29	22	-2.41	-0.95	350.7	782.0	47.8
J1441+3637	+296	17.1	12.2	4.60	**6**	**-25.42**	**18.61**	917.6	1 122.5	9.4

For J1205+4804, J1319-0114 and J1441+3637, which belong to the nearest stars, the assumption that the stars originate in the Galactic center leads to the very high proper motions $|\vec{\mu}|/(\text{mas yr}^{-1})$ of 84.7, 32.8 and 31.5. Due to this large proper motion, their space velocity would be larger than 840 $\frac{\rm km}{\rm s}$ and their ejection velocity would be larger than 1 000 $\frac{\rm km}{\rm s}$. Further stars with $|\vec{\mu}| > 10$ mas/yr are J0826+0734, J0905+0747, J0845+0836 and J0854+3217, with $|\vec{\mu}|/(\text{mas yr}^{-1}) = 21.2$, 15.0, 13.5 and 10.4.
Unfortunately, such high proper motions are not reported for any of these stars. One can conclude, that they don't come from the Galactic center or that they were involved in interactions which changed their direction of flight.

There are no other stars from this sample, whose ejection velocities are larger than the escape velocity at the Galactic center $v_{\rm esc}(\vec{0}) = 828\,\frac{\rm km}{\rm s}$ (see section 3.2), but many are only slightly below the escape-threshold according to this computation, so they still might be unbound, as their distance has not yet been determined very accurately.

4 Other models for the Galactic potential

4.1 Modified halo contribution in the potential of Allen & Santillán

In order to investigate the importance of the exact Galactic potential, former calculations have been repeated with modified parameters for the halo-potential Φ_3 in equation 2, namely $M_3' = 0$ and $M_3'' = 2M_3$.

Table 9: results for HVS4 in 75 kpc and 25 kpc distance with different halo-parameters in eq. 2

$d_{\rm HVS4}$	f	$M_3' = 0$	M_3	$M_3'' = 2M_3$	$\frac{f(M_3')}{f(M_3)}$	$\frac{f(M_3'')}{f(M_3)}$
75 kpc	μ_α/(mas/yr)	-0.157747	-0.156883	-0.156334	1.0055	0.9965
	μ_δ/(mas/yr)	-0.599348	-0.599548	-0.599439	0.9997	0.9998
	v/(km/s)	560.2	560.2	560.2	1.0000	1.0000
	$v_{\rm ej}$/(km/s)	865.5	951.9	1031.1	0.909	1.083
	T/Myr	137.1	128.4	121.6	1.068	0.947
25 kpc	μ_α/(mas/yr)	-1.058819	-1.055172	-1.051926	1.0035	0.9969
	μ_δ/(mas/yr)	-1.691979	-1.693287	-1.692418	0.9992	0.9995
	v/(km/s)	570.1	570.0	570.0	1.0002	1.0000
	$v_{\rm ej}$/(km/s)	863.3	918.5	970.5	0.940	1.057
	T/Myr	51.3	49.1	47.2	1.045	0.961

The main effect of the modified halo potential is on the ejection velocities and on the travel times: If the decelerating gravity of the halo was stronger ($M_3'' = 2M_3$), HVS4 would have to be ejected at a higher velocity (+8.3% for $d = 75$ kpc; +5.7% for $d = 25$ kpc) at the Galactic center to reach its current position with the measured radial velocity; its travel time would therefore be shorter (−5.3% for $d = 75$ kpc; −3.9% for $d = 25$ kpc) – and vice versa for lower halo mass ($M_3' = 0$). This effect is larger, if larger distances are assumed, see table 9.

Figures 14 and 15 show the space velocity as a function of time (assumed distances $d_{\mathrm{HVS4}} = 75$ kpc and $d_{\mathrm{HVS4}} = 25$ kpc) for the different potentials ($M_3' = 0$, M_3, $M_3'' = 2M_3$). Each plot starts at the ejection in the Galactic center.

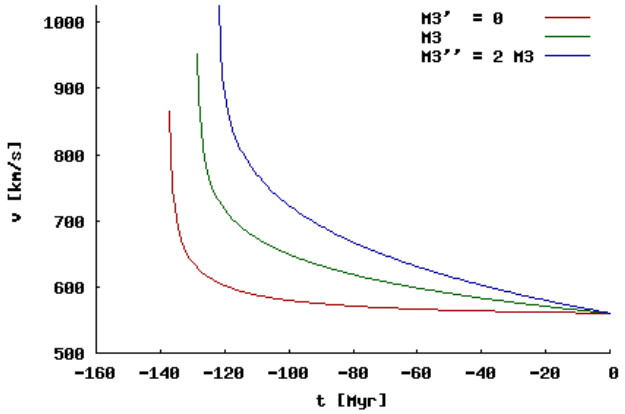

Figure 14: space velocity for different potentials, assuming $d_{\mathrm{HVS4}} = 75$ kpc

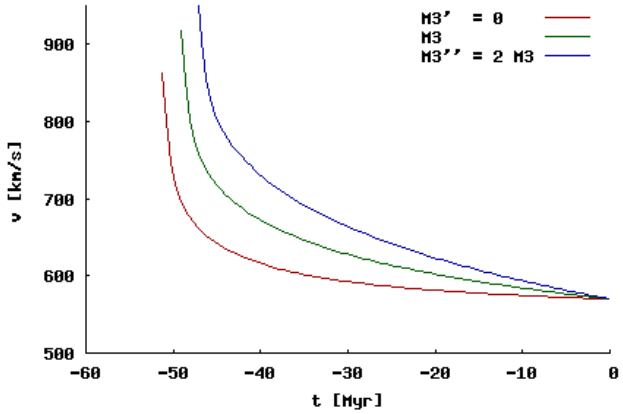

Figure 15: space velocity for different potentials, assuming $d_{\mathrm{HVS4}} = 25$ kpc

4.2 Simple model of Bromley for the Galactic center

In a recent paper [15], Bromley et al. want to calculate the spectrum of HVSs produced by the central black hole by disruption of binary stars. They use a "simple parameterization of the distribution of mass in the Galaxy":

$$\varrho(r) = \frac{\varrho_0}{1 + (\frac{r}{a_c})^\alpha} \quad ,$$

where $\alpha \approx 2$, the core radius is $a_c = 8$ pc and $\varrho_0 = 1.27 \cdot 10^4 \frac{M_\odot}{\mathrm{pc}^3}$. This spherical symmetric density leads to the potential

$$\Phi(r) = -\frac{GM(r)}{r} \qquad \text{with} \qquad M(r) = \int_{r' \le r} d^3\vec{r}\,' \, \varrho(\vec{r}\,') \;\; = \;\; 4\pi \int_0^r dr' \, \frac{r'^2 \, \varrho_0}{1 + (\frac{r'}{a_c})^\alpha}$$

For $\alpha = 2$, the mass function and therefore the potential can be evaluated analytically:

$$\alpha = 2 \quad \Rightarrow \quad M(r) = 4\pi\varrho_0 \, a_c^3 \left(\frac{r}{a_c} - \arctan(\frac{r}{a_c}) \right) \quad \Rightarrow \quad \Phi(r) \;\; = G \cdot 4\pi\varrho_0 \, a_c^2 \left(\frac{a_c}{r} \arctan(\frac{r}{a_c}) - 1 \right)$$

This spherical symmetric potential, which does not contain any disk contribution at all, would really be a extremely simple parameterization of the Galactic potential, if it was meant to describe the whole Galaxy. But one can infer from $M(r) \sim r$ for $r \gg a_c$, that it describes only its central region. Moreover, the potential first decreases with increasing distance from the Galactic center and then saturates at $-G \cdot 4\pi\varrho_0 \, a_c^2 = -44166 \, \frac{\mathrm{km}^2}{\mathrm{s}^2}$ (see figure 16), which would be counterintuitive.

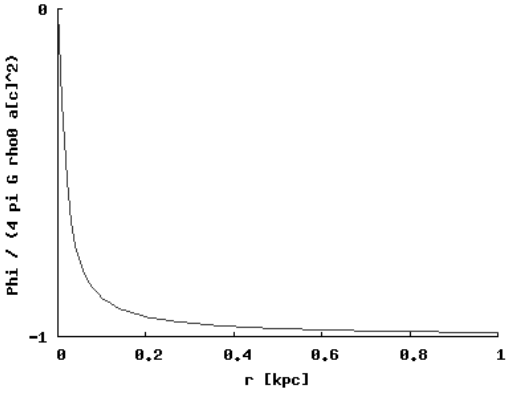

→ Figure 16: Galactic potential after Bromley

Therefore, this potential cannot be used to trace the HVSs back to the Galactic center.

4.3 Potential of Harding et al.

Other recent papers cite Harding et al. [16], who uses the Galactic potential $\Phi(\rho, z) = \Phi_{\mathrm{disk}}(\rho, z) + \Phi_{\mathrm{spher}}(r) + \Phi_{\mathrm{halo}}(r)$, which consists of the following Miyamoto-Nagai disk-potential, Hernquist spheroid- and logarithmic halo-potential:

$$\Phi_{\mathrm{disk}} = -\frac{GM_{\mathrm{disk}}}{\sqrt{\rho^2 + (a + \sqrt{z^2 + b^2})^2}} \, , \qquad \Phi_{\mathrm{spher}} = -\frac{GM_{\mathrm{spher}}}{r + c} \, , \qquad \Phi_{\mathrm{halo}} = v_{\mathrm{halo}}^2 \ln\left(\frac{r^2 + d^2}{\mathrm{kpc}^2} \right) \, ,$$

with following parameters: $M_{\mathrm{disk}} = 1.0 \cdot 10^{11} \, M_\odot = 4\,310 \, M_{\mathrm{gal}}$, $M_{\mathrm{spher}} = 3.4 \cdot 10^{10} \, M_\odot = 1\,466 \, M_{\mathrm{gal}}$, $v_{\mathrm{halo}} = 128 \, \frac{\mathrm{km}}{\mathrm{s}}$, $a = 6.5\,\mathrm{kpc}$, $b = 0.26\,\mathrm{kpc}$, $c = 0.7\,\mathrm{kpc}$, $d = 12.0\,\mathrm{kpc}$.

For the equations of motion, one needs the partial derivatives of the potential:

$$\frac{\partial\Phi}{\partial\rho} = \frac{GM_{\rm disk}\cdot\rho}{\left[\rho^2+(a+\sqrt{z^2+b^2})^2\right]^{3/2}} + \frac{GM_{\rm spher}\cdot\rho}{(r+c)^2\cdot r} + \frac{2v_{\rm halo}^2\cdot\rho}{r^2+d^2}$$

$$\frac{\partial\Phi}{\partial z} = \frac{GM_{\rm disk}\cdot(a+\sqrt{z^2+b^2})\cdot z}{\left[\rho^2+(a+\sqrt{z^2+b^2})^2\right]^{3/2}\cdot\sqrt{z^2+b^2}} + \frac{GM_{\rm spher}\cdot z}{(r+c)^2\cdot r} + \frac{2v_{\rm halo}^2\cdot z}{r^2+d^2}$$

If one repeats the analysis of the HVSs, the proper motions (which were found such that the trajectory comes from the Galactic center) deviate at most by 0.4% from those in in section 3.2, see figure 17 – they essentially make the space velocity vector direct to the Galactic center.
The same holds true for the current space velocity (figure 18), as it is determined by the radial velocity, which is fixed anyway, and by the proper motion and the distance, which are the same in both cases.

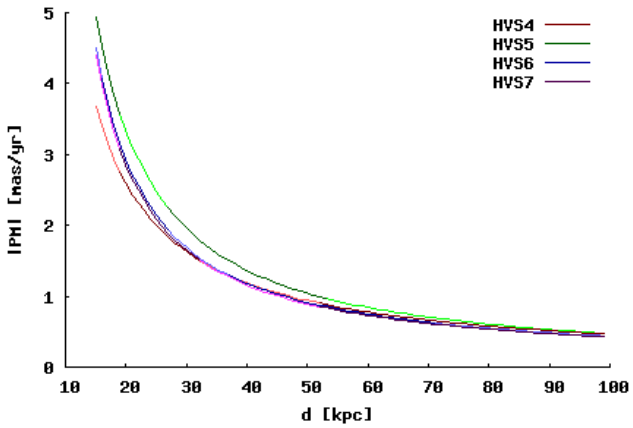

Figure 17: proper motions of the HVSs, predicted by the potential of Harding et al.

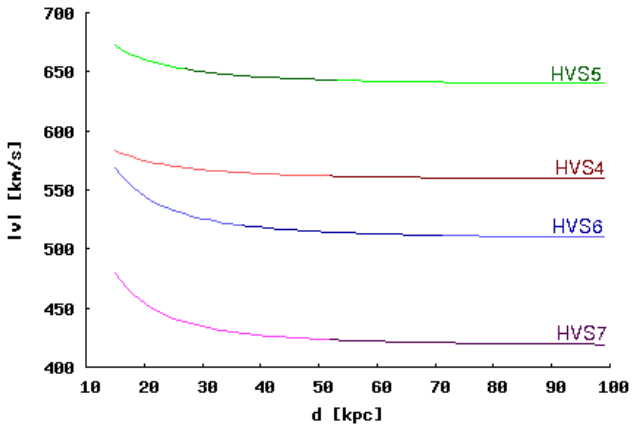

Figure 18: current space velocities of the HVSs, predicted by the potential of Harding et al.

The ejection velocities (figure 19) are however by up to 4.6% larger than in the computation with the potential of Allen & Santillán (section 3.2). The fact that ejection velocities do not form a very smooth line indicates, that the actual distance to the Galactic center (the program requires less than 10 pc) has stronger influence for this potential than for the other. So the code should actually be changed for this case.
Unfortunately, one cannot calculate escape velocities without giving an explicit cutoff for the dark halo potential of Harding et al., as $\lim_{r\to\infty}\Phi(\rho,z)\neq 0$ due to the (formally) confining $\Phi_{\rm halo}(r)\sim\ln(r)$. (In fact, $\Phi(\rho>4.3\,{\rm kpc},\ z=0)>0$, but Allen & Santillán's potential is (formally) confining as well: $\Phi(\rho,z)<0$ only for $\rho<273$ kpc.) This potential seems nevertheless appropriate at least for distances $r<100$ kpc, as this analysis of the HVSs gives the same results.

Due to the slightly larger ejection velocities, the travel times (figure 20) are by up to 1.3% shorter.

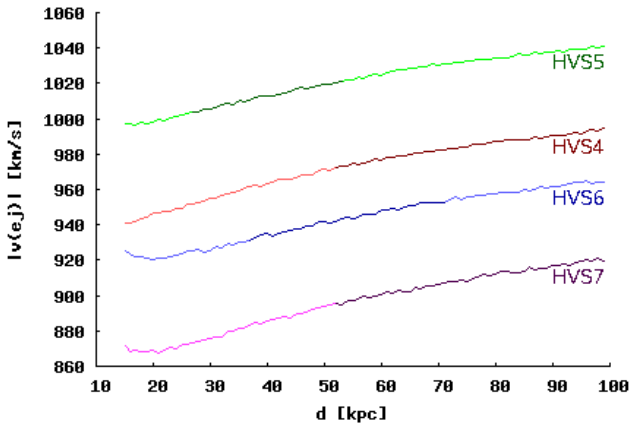

Figure 19: ejection velocities of the HVSs, predicted by the potential of Harding et al.

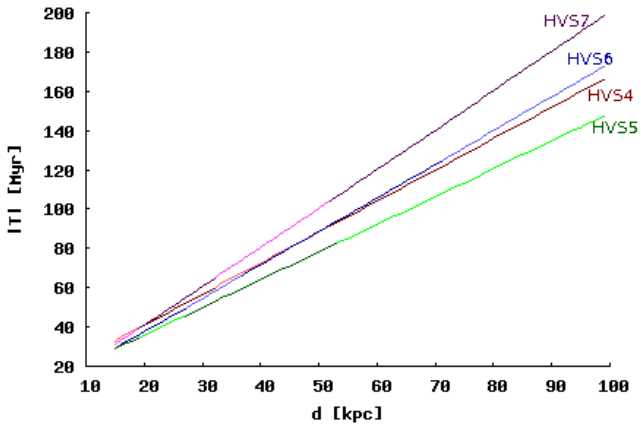

Figure 20: travel times of the HVSs, predicted by the potential of Harding et al.

From the kinematics of the HVSs #4 – #7, it is hard to distinguish between the model for the Galactic potential of Harding et al. and that of Allen & Santillán.

4.4 Potential of Flynn et al.

The potential $\Phi = \Phi_{_H} + \Phi_{_C} + \Phi_{_D}$ used by Flynn et al. [17] consists also of a logarithmic halo-potential, a core-potential and a disk-potential of Miyamoto-Nagai-type, but for core-/disk-potential, a combination of 2 or even 3 sets of parameters is used:

$\Phi_H(r) = \frac{1}{2} v_H^2 \ln\left(\frac{r^2 + r_0^2}{\mathrm{kpc}^2}\right)$	$v_H = 220\,\frac{\mathrm{km}}{\mathrm{s}}$	$r_0 = 8.5\,\mathrm{kpc}$
$\Phi_C(r) = \sum_{i=1}^{2} \frac{-GM_{C_i}}{\sqrt{r^2 + r_{C_i}^2}}$	$M_{C_1} = 3.0 \cdot 10^9\, M_\odot = 129.3\, M_{\mathrm{gal}}$ $M_{C_2} = 1.6 \cdot 10^{10}\, M_\odot = 689.7\, M_{\mathrm{gal}}$	$r_{C_1} = 2.7\,\mathrm{kpc}$ $r_{C_2} = 0.42\,\mathrm{kpc}$
$\Phi_D(\rho, z) = \sum_{i=1}^{3} \frac{-G \cdot M_{D_i}}{\sqrt{\rho^2 + (a_i + \sqrt{z^2 + b^2})^2}}$	$M_{D_1} = 6.6 \cdot 10^{10}\, M_\odot = 2845\, M_{\mathrm{gal}}$ $M_{D_2} = -2.9 \cdot 10^{10}\, M_\odot = -1250\, M_{\mathrm{gal}}$ $M_{D_3} = 3.3 \cdot 10^9\, M_\odot = 142.2\, M_{\mathrm{gal}}$	$a_1 = 5.81\,\mathrm{kpc}$ $a_2 = 17.43\,\mathrm{kpc}$ $a_3 = 34.86\,\mathrm{kpc}$ $b = 0.3\,\mathrm{kpc}$

The proper motions (figure 21) are again the same as in section 3.2 or 4.3: the deviations from the result for the potential of Allen & Santillán are only from -1.3% to +0.1%. The current space velocity (figure 22) is still less dependent, it differs at most by 0.3%.

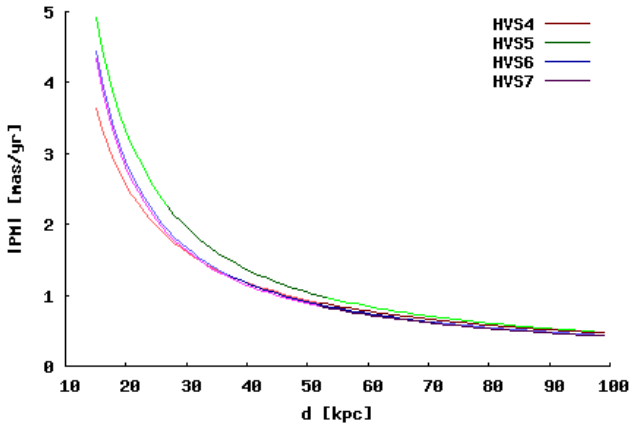

Figure 21: proper motions of the HVSs, predicted by the potential of Flynn et al.

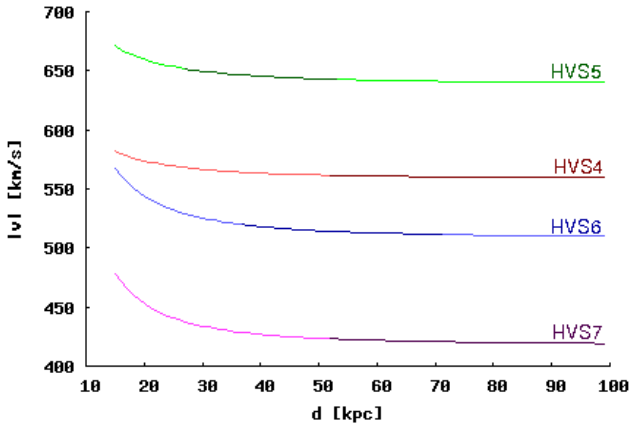

Figure 22: current space velocities of the HVSs, predicted by the potential of Flynn et al.

The ejection velocities (figure 23) are at most by 4.4% larger. As already stated for the potential of Harding et al. in section 4.3, one cannot calculate escape velocities, as $\Phi(\infty) = \infty$ due to the (formally) confining logarithmic dark halo potential, without introducing an explicit cutoff (such that $\Phi(\infty) < \infty$).
The travel times (figure 24) are again slightly shorter, namely by up to 4.5%, than those computed from the potential of Allen & Santillán in section 3.2.

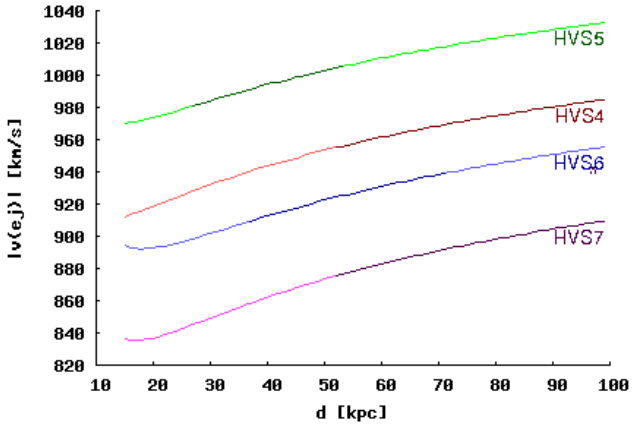

Figure 23: ejection velocities of the HVSs, predicted by the potential of Flynn et al.

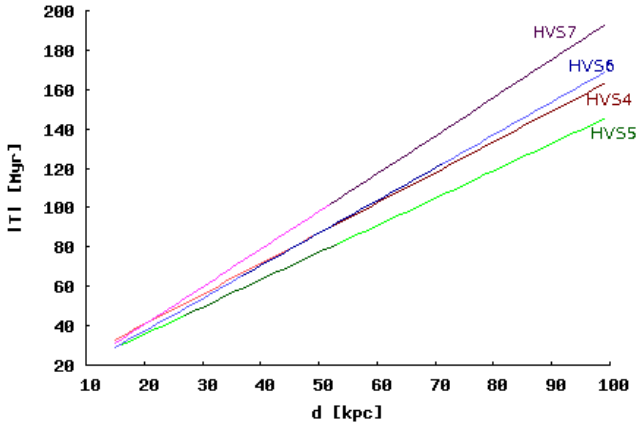

Figure 24: travel times of the HVSs, predicted by the potential of Flynn et al.

As a result, the potential of Flynn et al. describes the HVSs as well as those of Allen & Santillán and Harding et al.. These models of the Galactic potentials cannot be distinguished by current measurements on HVSs, and this situation also won't change in the near future.

5 Summary and conclusions

In the introductory section of this project, it was explained what hypervelocity stars are, how they possibly originate from the supermassive black hole in the Galactic center and which HVSs have been discovered yet. Their stellar types, distances and kinematics are not well known, especially for the latest HVSs, which can be either main sequence stars or horizontal branch stars.
Therefore, it was shown in section 2, how and which distances and maximal ages can be determined for HVS4 – HVS7 within different scenarios (main sequence stars with different metalicities or horizontal branch stars). If the HVS are MS stars, their distance is relatively large (and increases with the metalicity), but there is only a certain maximal age possible (which decreases with metalicity). Being HB stars, the HVSs could be relatively near, but very old.
In sections 3 and 4, a numerical code was used to determine kinematic parameters of the HVSs, provided that they really originate from the Galactic center: The necessary proper motions, velocities, escape velocities and travel times were discussed in great detail in section 3, while different models for the Galactic potential were investigated in section 4. It was shown that the proper motions of the HVSs are too low to be currently measurable. All HVSs are unbound to the Galaxy. The investigation of the travel times for HVS4 and HVS7 shows a tight balance with their own age, which may lead to the conclusion, that these HVSs had to be accelerated by the Galactic black hole soon after their birth near the central region of the Milky Way. But it is still possible, that HVS4 - HVS7 are all young main sequence stars which may have reached their current position (which is even not yet exactly known) within their lifetime.
The different Galactic potentials of Allen & Santillán, Harding et al. and Flynn et al. lead to the same results on the kinematics of the HVS within few percent and thus cannot be distinguished experimentally by means of these HVSs.

```
-----
| Mh
```

References

[1] Hills: "Hyper-velocity and tidal stars from binaries disrupted by a massive Galactic black hole", 1988, Nature, 331, 687-689

[2] Yu, Tremaine: "Ejection of Stars by Galactic Center Black Holes", 2003, ApJ, 599, 1129

[3] Brown et al.: "Discovery of an Unbound Hyper-Velocity Star in the Milky Way Halo", 2005, ApJ, 622, L33

[4] Edelmann et al.: "HE 0437-5439: An Unbound Hypervelocity Main-Sequence B-Type Star", 2005, ApJ, 634, L181

[5] Hirsch et al.: "US 708 - an unbound hyper-velocity subluminous O star", 2005, A&A 444, L61-L64

[6] Brown et al.: "A Successful Targeted Search for Hypervelocity Stars", 2006, ApJ, 640, L35-L38

[7] Brown et al.: "Hypervelocity Stars. I. The Spectroscopic Survey" 2006, ApJ, 647, 303-311

[8] Kurucz: "Model Atmospheres for G, F, A, B and O Stars", 1979, ApJ Supplement Series, 40, 1-340

[9] Landolt-B"ornstein: "Numerical Data and Functional Relationships in Science and Technology, Vol. 2: Astronomy and Astrophysics"

[10] Schaller et al.: "New grids of stellar models from 0.8 to 120 solar masses at Z = 0.020 and Z = 0.001", 1992, A&AS, 96, 269-331

[11] Schaerer et al.: "Grids of stellar models. II - From 0.8 to 120 solar masses at Z = 0.008", 1993, A&AS, 98, 523

[12] Schaerer et al.: "Grids of Stellar Models - Part Four - from 0.8-SOLAR-MASS to 120-SOLAR-MASSES at Z=0.040", 1993, A&AS, 102, 339

[13] Odenkirchen, Brosche: "Orbits of galactic globular clusters", 1992, AN, 313, 690

[14] Allen, Santillán: "An improved model of the galactic mass distribution for orbit computations", 1991, RMxAA, 22, 255-263

[15] Bromley et al.: "Predicting the Spectrum of Ejection Velocities", 2006, arXiv:astro-ph/0608159

[16] Harding et al.: "Mapping the Galactic Halo III. Simulated Observations of Tidal Streams", 2001, AJ, 122, 1397

[17] Flynn et al.: "Kinematics of the outer stellar halo", 1996, MNRAS, 281, 1027